

Depinning transition of dislocation assemblies: pileup and low-angle grain boundary

Paolo Moretti

*Dipartimento di Fisica, Università "La Sapienza", P.le A. Moro 2, 00185 Roma, Italy and
Center for Materials Science and Engineering, University of Edinburgh,
King's Buildings, Kenneth Denbigh Building, Edinburgh EH93JL, UK*

M.-Carmen Miguel

*Departament de Física Fonamental, Facultat de Física,
Universitat de Barcelona, Av. Diagonal 647, E-08028, Barcelona, Spain*

Michael Zaiser

*Center for Materials Science and Engineering, University of Edinburgh,
King's Buildings, Sanderson Building, Edinburgh EH93JL, UK*

Stefano Zapperi

*INFM UdR Roma 1 and SMC, Dipartimento di Fisica,
Università "La Sapienza", P.le A. Moro 2, 00185 Roma, Italy*

We investigate the depinning transition occurring in dislocation assemblies. In particular, we consider the cases of regularly spaced pileups and low angle grain boundaries interacting with a disordered stress landscape provided by solute atoms, or by other immobile dislocations present in non-active slip systems. Using linear elasticity, we compute the stress originated by small deformations of these assemblies and the corresponding energy cost in two and three dimensions. Contrary to the case of isolated dislocation lines, which are usually approximated as elastic strings with an effective line tension, the deformations of a dislocation assembly cannot be described by local elastic interactions with a constant tension or stiffness. A nonlocal elastic kernel results as a consequence of long range interactions between dislocations. In light of this result, we revise statistical depinning theories and find novel results for Zener pinning in grain growth. Finally, we discuss the scaling properties of the dynamics of dislocation assemblies and compare theoretical results with numerical simulations.

I. INTRODUCTION

The depinning transition of individual dislocations gliding on their slip plane has been widely investigated in the past [1, 2, 3, 4, 5, 6] in order to explain solid solution hardening [7, 8, 9], that is, the increase of the yield stress value when solute atoms are present in a crystal. The presence of solute atoms changes the local properties of the host material, resulting in a pinning force on nearby dislocations [8, 9]. This is not the only source of pinning, which can also be provided by particle inclusions or by immobile dislocations in other inactive slip systems [7]. Several approximate calculations have been performed in the past to obtain the depinning stress from a statistical summation of individual pinning forces. In this respect, collective pinning theories have been very successful in the case of diffuse weak pinning forces [10, 11, 12], whereas the theory introduced by Friedel [13] is appropriate in the case of localized strong pinning centers.

From the purely theoretical point of view, dislocations provide a concrete example of a more general problem: that of driven elastic manifolds in quenched random media [14]. Apart from dislocations, other examples of this general problem are domain walls in ferromagnets [15, 16], flux lines in type II superconductors [17, 18], contact lines [19, 20], and crack fronts [21, 22]. In recent years, a vast theoretical effort has been devoted to

understand the depinning transition as a non-equilibrium critical phenomenon [14, 23, 24, 25, 26, 27, 28]. The morphology of a depinning manifold is generally found to be self-affine and can be characterized by a roughness exponent. Other scaling exponents have been introduced to characterize the behavior of correlation lengths and times, the velocity above depinning, and the avalanching motion observed as the critical threshold is approached. Quantitative predictions of the critical exponents have been obtained analytically by the renormalization group [14, 23, 24, 25, 26, 27, 28], and have been confirmed by numerical simulations [24, 29, 30, 31, 32, 33, 34, 35]. In the course of time, a deeper level of description and understanding of this phenomenon has been achieved, going far beyond a mere estimate of the depinning force, which has typically been the original motivation to address the problem.

The analysis of the depinning transition in dislocation theory has often been made in the approximation of a dislocation line tension [1, 2, 3, 4, 5]. Hence, a dislocation is considered to be a flexible string with a constant line tension. This analogy is not fully accurate. In fact, the bending of a dislocation produces long-range stress and strain fields [36, 37] such that the self-energy of a dislocation line segment depends on its interaction with all the other segments on the line, and therefore depends of the particular dislocation configuration. Long range in-

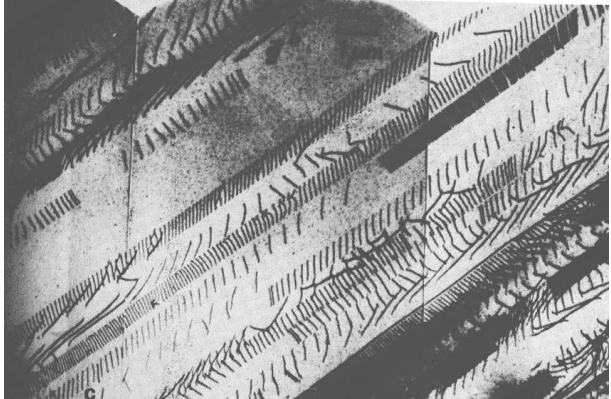


FIG. 1: Transmission electron micrograph taken from a Cu-14.4at%Al single crystal deformed at room temperature; the image shows large regularly spaced dislocation pile-ups. Courtesy of J. Plessing and H. Neuhäuser [44].

teractions lead to a wavevector-dependent effective line tension. This is also well-known in the case of vortex lines in high temperature superconductors [38] or, for instance, for a dislocation line in a vortex crystal [39]. In spite of this wavevector dependence, the main features of the depinning transition are basically unchanged [6], due to the fact that this effective line tension is only varying logarithmically with the wavevector. Numerical simulations indicate, however, a slight difference in the roughness exponent in the two cases which, at present, is still not well understood [6, 34]. A similar surface tension approximation is also used in the theory of Zener pinning [40, 41], to describe the interactions between grain boundaries and solute atoms during grain growth [42].

While the behavior of an isolated dislocation pushed through a random distribution of obstacles is at present quite well understood, the results do not necessarily carry over to the more realistic case of collective dislocation motion. Dislocations interact via their long-range stress fields, which may induce intriguing jamming and avalanche-like phenomena even in the absence of quenched pinning centers [43]. In most cases, one can not simply neglect interactions and treat dislocations as isolated objects. The depinning transition of interacting dislocation lines and/or loops of generic orientations and Burgers vectors in a random solute distribution seems to be a formidable task for theoretical treatment. In several instances, however, dislocations are arranged into regular structures that are amenable to a theoretical treatment. In particular, here we analyze the depinning transition of regularly spaced pileups and low angle grain boundaries (LAGB). These relatively simple structures are sometimes observed experimentally (see Fig. 1) and provide a nice illustration of the effect of dislocation interactions on the depinning transition. An early analysis of the depinning of a dislocation pileup was presented in Ref. [45], considering explicitly the emission of dislocations from a source.

Here we address the problem by first computing the stress and elastic energy associated to a small deformation of the dislocation structure. This allows us to assess the validity of a local tension approximation, which turns out to be completely inadequate in this context. Long-range interactions between the dislocations involved give rise to much larger self-stresses than for isolated dislocations. As a result, pileups and low angle grain boundaries are much stiffer than single dislocations. The elastic energy is then used in the framework of statistical pinning theories to estimate the depinning stress. In particular we consider collective pinning theory and Friedel statistics. As an application of these results, we revise the theory of Zener pinning in grain growth which originally made use of a surface tension approximation for the elastic self-stress. The correct treatment of long-range stresses and dislocation interactions inside the grain boundary yields a different result for the dependence of grain size on material parameters.

At stresses close to the depinning stress, the dynamics of the dislocation structures we are investigating exhibits critical behavior which can be characterized in terms of scaling exponents. Using previous renormalization group results, we gain a complete quantitative picture of the depinning transition. In the elastic approximation, pileups and low angle grain boundaries are equivalent to a standard interface depinning problem with long-range elasticity. In two dimensions, the problem can be mapped to a contact line or to a planar crack, which have been extensively studied in the literature. In three dimensions, the self-stress is similar to the dipolar force in magnetic domain walls and leads to logarithmically rough deformations. In more technical terms, $d = 3$ is the upper critical dimension for the transition, which is well described by mean-field exponents, up to logarithmic corrections.

The scaling exponents associated with the depinning transition describe not only the morphology of the dislocation assembly but also its dynamics. In order to confirm the validity of the elastic calculations, on which we based the mapping with elastic manifolds, we perform a series of numerical simulations for a dislocation pileup. We consider a two dimensional system, neglecting the deformation of single dislocations, which amounts to an effective one dimensional particle model. Simulations of the model display results in agreement with the theory and allow to illustrate some interesting dynamical effects. In particular, the pileup displays a zero temperature power law creep relaxation which can be interpreted by scaling relations. Below threshold, the power law relaxation terminates into a pinned configuration, while above threshold there is a crossover to linear creep or average constant velocity sliding. As it is common for this class of systems, the motion of the pileup takes places in the form of avalanches whose distribution again can be characterized by scaling exponents.

II. ELASTICITY

Developing a theory for collective dislocation depinning requires the basic knowledge of the elastic properties of the dislocation assembly in the first place. In this section, we determine the elastic response of two particular dislocation assemblies: a regularly spaced pileup and a low angle grain boundary of edge dislocation lines. The two structures are quite similar geometrically; they are both one-dimensional arrangements of N dislocation lines with the same Burgers vector \mathbf{b} and average line direction \hat{e} (for edge dislocations $\hat{e} \perp \mathbf{b}$) along a given direction of space \hat{d} , but they differ in the relative orientation of the Burgers vector and the arrangement direction \hat{d} . In particular, in a pileup a set of edge dislocations lies in the slip plane, defined by the dislocations axis \hat{e} and the Burgers vector, so that $\hat{d} \parallel \hat{b}$ (see Fig. 2 for a particular example with $\hat{e} = \hat{z}$ and $\hat{d} \parallel \hat{b} \parallel \hat{y}$), while in the LAGB the edge dislocations lie in the perpendicular plane such that $\hat{d} \perp \hat{b}$ (see Fig. 3 for a particular geometry). Neglecting climb, i.e. the motion of a dislocation perpendicular to its slip plane, deformations of the structure occur solely within the slip plane both for the pileup and for the LAGB. In this section we derive the shear stress and the elastic energy associated with small deformations of these dislocation assemblies. This is needed in order to derive the yield stress from statistical pinning theories. For completeness, we consider the problem both in two and in three dimensions.

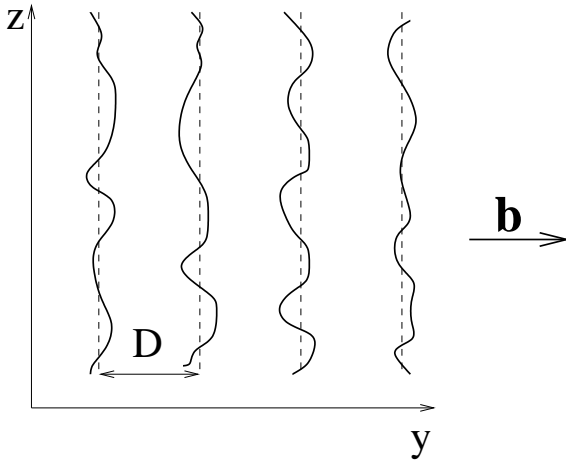


FIG. 2: A regularly spaced dislocation pileup with Burgers vector along the y axis. The ideal configuration is plotted with straight dashed lines, whereas the solid lines represent their possible glide deformations within the slip plane yz .

A. Two dimensions

In this particular case, we do not consider elastic deformations along the dislocation line direction. This approximation is relevant for thin crystals and amounts to treat the dislocations in the structure as rigid lines, rendering a two-dimensional problem. On the other hand, we take into account small variations in the position of the dislocations in the one-dimensional structures they form. We consider the case of LAGB and then directly extend the result to the pileup case. In fact, in linear approximation the elastic energy turns out to be the same in both cases.

Here and throughout the paper, we consider an ideal LAGB as an infinite set of equally spaced edge dislocations lying on the yz plane (without loss of generality we consider the plane $x = 0$) with Burgers vector pointing along the positive x axis $\mathbf{b} = b\hat{x}$ (see Fig. 3). In the rigid dislocation approximation, we do not consider the deformations along the z axis so that each dislocation is described by a set of coordinates (x_n, y_n) , where $y_n = nD$, D is the grain boundary spacing, and where x_n is a small displacement from the $x = 0$ plane. The shear stress field at a given point (x, y) due to a dislocation at (x_n, y_n) is given by [13, 46]

$$\sigma_{xy}^n(x, y) = \frac{\mu b}{2\pi(1-\nu)} \frac{(x - x_n)[(x - x_n)^2 - (y - y_n)^2]}{[(x - x_n)^2 + (y - y_n)^2]^2} \quad (1)$$

where μ is the shear modulus and ν is the Poisson ratio. The glide component of the total force per unit length on another dislocation m in the LAGB can be readily obtained from the Peach-Koehler expression $\mathbf{f} = (\sigma \cdot \mathbf{b}) \times \hat{e}$ [13, 46]

$$f_x(x_m, y_m) = b \sum_{n=-\infty}^{+\infty} \sigma_{xy}^n(x_m, y_m). \quad (2)$$

For small deformations $|x_m - x_n| \ll D|m - n|$ we have

$$f_x(x_m, y_m) = -\frac{\mu b^2}{2\pi(1-\nu)} \sum_{n=-\infty}^{+\infty} \frac{x_m - x_n}{(y_m - y_n)^2}, \quad (3)$$

which can be used to obtain the elastic energy

$$E = - \sum_{m=-\infty}^{+\infty} \int f_x(x_m, y_m) dx_m = \frac{\mu b^2}{8\pi(1-\nu)} \sum_{m=-\infty}^{+\infty} \sum_{n=-\infty}^{+\infty} \frac{(x_m - x_n)^2}{(m - n)^2 D^2} \text{ with } m \neq n. \quad (4)$$

It is instructive to express the elastic energy in Fourier space, where one can easily identify the energy cost of the different modes. For an infinitely long LAGB $N \rightarrow \infty$, we can write the dislocation displacements as

$$x_m = \int_{BZ} \frac{dk}{2\pi} e^{-ikDm} x(k), \quad (5)$$

where the integral is restricted to the first Brillouin zone (BZ) of the reciprocal space, and using the following results

$$\sum_{d=1}^{+\infty} \frac{1}{d^2} = \frac{\pi^2}{6}, \quad \sum_{d=1}^{+\infty} \frac{\cos(\gamma d)}{d^2} = \frac{\pi^2}{6} - \frac{\pi|\gamma|}{2} + \frac{\gamma^2}{4} \quad (6)$$

we obtain [47]

$$E = \frac{\mu b^2}{8\pi(1-\nu)D^2} \int_{BZ} \frac{dk}{2\pi} (2\pi|k| - Dk^2) \tilde{x}(k) \tilde{x}(-k). \quad (7)$$

From this expression, one can see that the elastic interaction kernel $(2\pi|k| - Dk^2)$ is not quadratic in the wavevector, as it would be the case for a local elastic manifold with a constant tension or stiffness, but grows roughly as $|k|$ for long wavelength deformations. This is a consequence of long range interactions between dislocations in the LAGB which render a much stiffer structure. In the following sections we will explore the relevant consequences of this result in the collective depinning of such dislocation structures, something that has been disregarded in previous dislocation depinning studies.

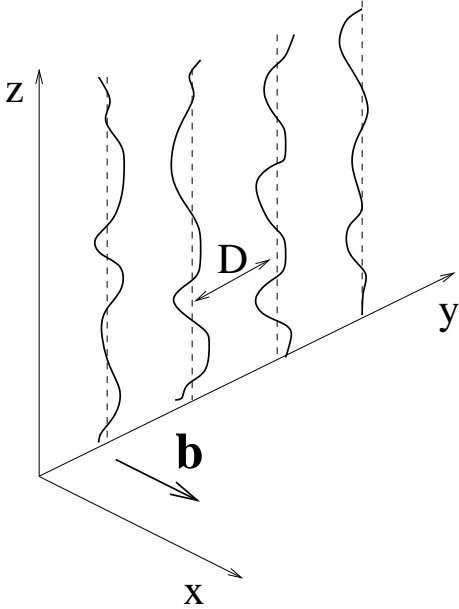


FIG. 3: A regularly spaced low angle grain boundary where the dislocations Burgers vector is parallel to the x axis. The ideal configuration is plotted with straight dashed lines in the plane yz , whereas the solid lines represent their possible glide deformations within the slip plane xz .

The elastic energy associated with perturbations of a regularly spaced dislocation pileup can be obtained in an analogous manner. According to the geometric conditions assumed here, all Burgers vectors are now oriented along the positive y axis, and since the dislocations are all in the same slip plane we can now write $x = x_n = 0$. Proceeding as before, the total Peach-Koehler force on dislocation m along the new glide direction is given by

$$f_y(0, y_m) = \frac{\mu b^2}{2\pi(1-\nu)} \sum_{n=-\infty}^{+\infty} \frac{1}{y_m - y_n}. \quad (8)$$

Notice that the Peach-Koehler force is now repulsive, however the stability of the system is ensured in the case of an infinite pileup where the dislocations located at the extremes (at $\pm\infty$) have fixed positions, or equivalently, for a finite pileup with periodic boundary conditions. Thus one can also compute the elastic energy cost of small displacements δy_m of the dislocations in the pileup with respect to their stable positions. Up to first order in δy_m , we obtain a recovery elastic force

$$f_y(0, \delta y_m) = -\frac{\mu b^2}{2\pi(1-\nu)} \sum_{n=-\infty}^{+\infty} \frac{\delta y_m - \delta y_n}{(y_m - y_n)^2} \quad (9)$$

equivalent to the one obtained for the case of the LAGB. The corresponding elastic energy cost

$$\tilde{E} = \frac{\mu b^2}{8\pi(1-\nu)D^2} \int_{BZ} \frac{dk}{2\pi} (2\pi|k| - Dk^2) \delta y(k) \delta y(-k) \quad (10)$$

has the same form with a long-range interaction kernel. Thus as a partial conclusion of this section, we can emphasize that long wavelength distortions of low angle grain boundaries and equally spaced pileups of straight dislocation lines with translational invariance along the dislocation axis have the same nonlocal elastic properties, with eigenvalues that grow linearly with the modulus of the wavevector considered.

B. Three dimensions

In this section, we consider the more general and realistic case of deformable dislocation lines where, according to the geometry established in the previous section, we loose the translational invariance along the z axis. As before, we consider first the case of a LAGB with Burgers vectors oriented along the x axis, in which each dislocation can be described by a set of coordinates $(x_n(z), y_n, z)$, where again $y_n = nD$, but where now the displacement $x_n(z)$ with respect to the $x = 0$ plane depends on the height of the infinitesimal dislocation segment considered (see Fig. 3). The elastic stress field due to a general dislocation line or loop can be obtained, for instance, by considering the line as being composed of elementary segments of infinitesimal length [46]. Depending on the relative orientation of the Burgers vector and

the local tangent vector $\hat{\tau}(z)$, each segment can either have edge ($\hat{\tau}(z) \perp \mathbf{b}$) or screw character ($\hat{\tau}(z) \parallel \mathbf{b}$), or it can be a combination of both. A first approximation of a general dislocation line can be its parametrization in terms of a succession of only edge and screw segments [48]. The mathematical form of the elastic stress fields generated by these two types of elementary segments is simpler and renders amenable the analytic treatment of the problem. For instance, the shear stress field due to an edge dislocation segment of length $\Delta z'$ and located at the point (x', y', z') is given by [46]

$$\sigma_{xy}(x, y, z) = \frac{\mu b}{4\pi(1-\nu)} \frac{x-x'}{R_0^3} \left[1 - 3 \frac{(y-y')^2}{R_0^2} \right] \Delta z', \quad (11)$$

where

$$R_0^2 = (x-x')^2 + (y-y')^2 + (z-z')^2. \quad (12)$$

On the other hand, the shear stress field due to an screw segment of length $\Delta x'$ is [46]

$$\sigma_{xy}(x, y, z) = -\frac{\mu b}{4\pi} \frac{z-z'}{R_0^3} \Delta x'. \quad (13)$$

Equations (11) and (13) allow us to calculate the glide component of the total Peach-Koehler force $\mathbf{f} = (\sigma \cdot \mathbf{b}) \times \hat{\tau}$

on an edge or an screw segment. The glide force on an edge segment at $(x_m(z), y_m, z)$ has two components due to any other edge f_x^{EE} or screw segments f_x^{SE}

$$\begin{aligned} f_x^{EE}(x_m(z), y_m, z) &= \frac{\mu b^2}{4\pi(1-\nu)} \frac{x_m(z) - x_n(z')}{R_{mn}^3(z, z')} \\ &\quad \left[1 - 3 \frac{(y_m - y_n)^2}{R_{mn}^2(z, z')} \right] \Delta z' \Delta z, \quad (14) \\ f_x^{SE}(x_m(z), y_m, z) &= -\frac{\mu b^2}{4\pi} \frac{z - z'}{R_{mn}^3(z, z')} \frac{\partial x_n(z')}{\partial z'} \Delta z' \Delta z, \end{aligned}$$

respectively. Note that up to first order in the small displacements ($x_m(z) - x_n(z') \simeq 0$), the relative distance among segments can be written as $R_{mn}^2(z, z') = (y_m - y_n)^2 + (z - z')^2$. On the other hand, from the general expression for the Peach-Koehler written above, it is straightforward to verify that there are no glide forces acting upon any screw segment on the dislocation line. After summing up all nonvanishing contributions, we can obtain the elastic energy as for the two dimensional case (see Eq.(4)). The elastic energy can be expressed as the sum $E = E^{EE} + E^{SE}$ of the interaction energies between edge-edge and edge-screw segments. These interaction energies are given by

$$E^{EE} = -\frac{\mu b^2}{32\pi(1-\nu)} \sum_{m,n} \int \int dz dz' \left[1 - 3 \frac{(y_m - y_n)^2}{R_{mn}^2(z, z')} \right] \frac{[x_m(z) - x_n(z')]^2}{R_{mn}^3(z, z')}, \quad (15)$$

$$E^{SE} = \frac{\mu b^2}{16\pi} \sum_{m,n} \int \int dz dz' \frac{z - z'}{R_{mn}^3(z, z')} x_m(z) \partial_{z'} x_n(z'). \quad (16)$$

As we did for the rigid line case, we can also express this elastic energy in Fourier space in order to diagonalize the interaction matrix and to obtain the wavevector dependence of the interaction kernel between the different deformation modes. The detailed calculation is rather lengthy, so we merely indicate the procedure followed and the final results obtained. We evaluate separately the energy contribution due to the self-interaction between the constituent segments of each individual dislocation line, i.e. $n = m$, which we denote by E_0 , and the energy contributions due to the interaction of dislocation segments

lying on different lines, i.e. $n \neq m$, which we refer to as E_1 . Proceeding this way, we find that the total energy is $E = E_0^{EE} + E_0^{ES} + E_1^{EE} + E_1^{ES}$. We express the dislocation displacements in terms of their Fourier modes,

$$x_m(z) = \int_{BZ} \frac{dk}{2\pi} \int \frac{dq}{2\pi} e^{-ikDm} e^{-iqz} x(k, q) \quad (17)$$

and evaluate the self-interaction contributions for long wavelength deformations $qa \ll 1$ where a is a short-distance cutoff introduced to preclude the interaction of a line segment with itself. The result can be written as

$$E_0^{EE} = \frac{\mu b^2}{16\pi(1-\nu)} \int_{BZ} \frac{dk}{2\pi} \int \frac{dq}{2\pi} \frac{1}{D} \left[2 \left(\gamma - \frac{3}{2} + \ln a|q| \right) q^2 - \frac{a^2}{12} q^4 \right] x(k, q) x(-k, -q) \quad (18)$$

$$E_0^{SE} = \frac{\mu b^2}{8\pi} \int_{BZ} \frac{dk}{2\pi} \int \frac{dq}{2\pi} \frac{1}{D} \left[2(-\gamma - \ln a|q|) q^2 + \frac{a^2}{2} q^4 \right] x(k, q) x(-k, -q) \quad (19)$$

where γ is the Euler constant. The usual quadratic wavevector dependence of a local interaction kernel is modified in this particular case by logarithmic corrections. This is known to be the result of long range interactions in the case of a dislocation line, as well as for

similar singularities such as vortex lines in high temperature superconductors [38].

Similarly, the energy contributions due to interactions between segments of different dislocation lines ($n \neq m$) in the LAGB can be expressed as

$$E_1^{EE} = \frac{\mu b^2}{16\pi(1-\nu)} \int_{BZ} \frac{dk}{2\pi} \int \frac{dq}{2\pi} \frac{1}{D} \left[2 \left(\gamma + \ln \frac{D|q|}{4\pi} \right) k^2 + \frac{2\pi}{D} \frac{k^2}{(k^2 + q^2)^{1/2}} + \frac{D^2}{2\pi^2} \zeta(3) k^2 q^2 \right] x(k, q) x(-k, -q) \quad (20)$$

$$E_1^{SE} = \frac{\mu b^2}{16\pi} \int_{BZ} \frac{dk}{2\pi} \int \frac{dq}{2\pi} \frac{1}{D} \left[2 \left(\gamma + \ln \frac{D|q|}{4\pi} \right) q^2 + \frac{2\pi}{D} \frac{q^2}{(k^2 + q^2)^{1/2}} + \frac{D^2}{2\pi^2} \zeta(3) q^4 \right] x(k, q) x(-k, -q), \quad (21)$$

where $\zeta(x)$ is the Riemann *zeta* function. Naturally, the interaction kernel between the deformation modes for the three dimensional grain boundary case depends explicitly on both the y and z components of the wavevector in an intricate manner. Nevertheless, as in the two dimensional case, for long wavelength deformations the leading term of the interaction kernel is essentially linear in the wavevector, which manifests the nonlocality of the interactions.

Finally, let us consider the case of a three dimensional pileup with the same geometric specifications as adopted in the rigid-line case (see Fig. 2). Since the Burgers vector is oriented along the y axis, the glide component of the Peach-Koehler force on screw segments (now parallel to the y axis) vanishes. On the other hand, there is a non-vanishing glide force on edge segments due to the shear stress field generated by any other segments. For instance, the shear stress field due to an edge dislocation segment of length $\Delta z'$ and located at the point (x', y', z') in this case is given by [46]

$$\sigma_{xy}(x, y, z) = -\frac{\mu b}{4\pi(1-\nu)} \frac{y - y'}{R_0^3} \left[1 - 3 \frac{(x - x')^2}{R_0^2} \right] \Delta z'. \quad (22)$$

Moreover, the shear stress generated by an screw segment of length $\Delta y'$ is [46]

$$\sigma_{xy}(x, y, z) = \frac{\mu b}{4\pi} \frac{z - z'}{R_0^3} \Delta y'. \quad (23)$$

Without loss of generality we consider a pileup lying on the $x = 0$ plane, and we account for small perturbations affecting the y_n coordinates of the dislocation lines in the ideal assembly. Thus, we can replace $y_m - y_n \rightarrow (y_m + \delta y_m(z)) - (y_n + \delta y_n(z'))$, where the displacements depend on the z coordinate of the infinitesimal line segment considered. Expanding up to first order in $(\delta y_m(z) - \delta y_n(z'))$, the resulting Peach-Koehler glide forces on an edge segment due to other edge f_y^{EE} or screw segments f_y^{SE} are

$$\begin{aligned} f_y^{EE}(0, y_m + \delta y_m(z)) &= \frac{\mu b^2}{4\pi(1-\nu)} \frac{\delta y_m(z) - \delta y_n(z')}{R_{mn}^3(z, z')} \left[1 - 3 \frac{(y_m - y_n)^2}{R_{mn}^2(z, z')} \right] \Delta z' \Delta z, \\ f_y^{SE}(0, y_m + \delta y_m(z)) &= -\frac{\mu b^2}{4\pi} \frac{z - z'}{R_{mn}^3(z, z')} \frac{\partial \delta y_n(z')}{\partial z'} \Delta z' \Delta z, \end{aligned} \quad (24)$$

where

$$R_{mn}^2(z, z') = (y_m - y_n)^2 + (z - z')^2. \quad (25)$$

The corresponding elastic energy is

$$E^{EE} = -\frac{\mu b^2}{32\pi(1-\nu)} \sum_{m,n} \int \int dz dz' \left[1 - 3 \frac{(y_m - y_n)^2}{R_{mn}^2(z, z')} \right] \frac{[\delta y_m(z) - \delta y_n(z')]^2}{R_{mn}^3(z, z')}, \quad (26)$$

$$E^{SE} = +\frac{\mu b^2}{16\pi} \sum_{m,n} \int \int dz dz' \frac{z - z'}{R_{mn}^3(z, z')} \delta y_m(z) \partial_{z'} \delta y_n(z'). \quad (27)$$

Proceeding along the same lines indicated in the case

of a LAGB, i.e. separating the intra-line interactions

from the inter-line ones, it can be expressed in terms of Fourier modes as $E = E_0^{EE} + E_0^{ES} + E_1^{EE} + E_1^{ES}$. The expressions turn out to be equal to the one obtained for the LAGB and can be recovered replacing $x(\pm k, \pm q)$ with $\delta y(\pm k, \pm q)$ in Eqs. 18-21.

Thus also in this case we find wavevector dependent interaction kernels whose leading terms (for low wavelength deformations) grow either linearly with the wavevector in the case of interline interactions, or quadratically with logarithmic corrections in the case of intraline interactions. We thus can conclude that this particular form of the elastic kernels is characteristic of the long range interactions between different dislocations. As we will see in the following, the long-range elastic properties preclude the analysis of the depinning transition of dislocation assemblies based upon a local theory with a constant effective stiffness.

III. DISORDER: DEPINNING TRANSITION

Distortions in a LAGB or a pileup arise from interactions of the dislocations with various kinds of impurities such as solute atoms, precipitates or other immobile defects. The interactions between individual dislocations and impurities have been computed and are reported in the literature. For the purpose of this article, we will consider quenched disorder created by a random distribution of immobile impurities with concentration c which interact with dislocations via a force $f_p(r) = f_0 g(r/\xi_p)$, where f_0 is the pinning strength, ξ_p is the interaction range and r is the distance between the impurity and the dislocation. The detailed shape $g(x)$ of the individual pinning force is inessential for most purposes.

The morphology and dynamics of a pileup or a LAGB result from a complicated interplay between elasticity and disorder. Pileup and LAGB are examples of the general problem of the depinning of elastic manifolds in random media, which has been extensively studied in the past [14]. In the elastic approximation, the dynamics of the pileup or the LAGB follows

$$\chi \frac{\partial u}{\partial t} = \int d^d x' K(x - x')(u(x') - u(x)) + b\sigma + \eta(x, u), \quad (28)$$

where χ is a damping constant, σ is the applied stress, $\eta(x, u)$ describes the effect of the pinning centers and the elastic interaction kernel K , computed in the previous section, scales as $|k|$ in Fourier space. In the following we will discuss how the main theoretical approaches to the depinning transition can be applied to the problem at hand.

A. Collective pinning theory: weak pinning

Collective pinning theory describes the behavior of an elastic manifold in the limit of weak disorder, when pinning is due to the fluctuations of the random forces. The

key concept is the introduction of a characteristic length L_c above which pinning becomes effective (or energetically advantageous) and consequently the manifold is distorted. The collective pinning length can be evaluated, for instance, by balancing the elastic energy cost and the pinning energy gain associated with a small displacement of a region of linear size L . On scales below L , the manifold remains essentially undeformed and, hence, the fluctuations in potential energy follow Poissonian statistics. The effective concentration of the pinning defects along the LAGB is given by

$$\bar{c}_{\text{eff}} = \begin{cases} \bar{c} & , \xi_p > D \\ \bar{c} \frac{\xi_p}{D} & , \xi_p < D \end{cases} \quad (2D) \quad (29)$$

$$c_{\text{eff}} = \begin{cases} c & , \xi_p > D \\ c \frac{\xi_p}{D} & , \xi_p < D \end{cases} ; (3D) .$$

The first expression refers to pinning by columnar defects of areal concentration \bar{c} in $d = 2$, and the second to pinning by localized defects of volume concentration c in $d = 3$. In $d=2$, the characteristic energy of a section of a LAGB of size L displaced by an amount of the order of u can be written as

$$\bar{E} = \frac{\mu b^2 u^2}{D^2} - \bar{f}_0 \xi_p \sqrt{\bar{c}_{\text{eff}} L u}. \quad (30)$$

Here both \bar{E} and \bar{f}_0 are defined as quantities per unit length. In the case of a thin film of thickness h , one can obtain their three-dimensional counterparts just as $E = h\bar{E}$ and $f_0 = h\bar{f}_0$. Note the scale-independence of the nonlocal expression of the elastic energy $\mu b^2 u^2 / D^2$ in contrast to what would be this energy in the local approximation $\mu b^2 u^2 / DL$. Essentially the same expression holds for the pileup. Balancing elastic and pinning contributions and imposing that the displacement is of the order of the pinning range $u \sim \xi_p$, one readily obtains $L_c = (\mu^2 b^4 \xi_p) / (D^4 f_0^2 \bar{c}_{\text{eff}})$. The LAGB is depinned when the work done by the external stress in moving a segment of length L_c over the distance ξ_p exceeds the characteristic pinning energy $\bar{E}(L_c)$ of this segment. Equating $\bar{E}(L_c) = \sigma_c b L_c \xi_p / D$, for the case above the result is given by $\sigma_c b = (\bar{c}_{\text{eff}} f_0^2 D^3) / (\mu b^2)$.

A similar calculation in $d = 3$ is more subtle, since the elastic and the pinning energies scale with the same power of L and thus cancel in the simple dimensional approach discussed above. As we will discuss in the next section, this reflects the fact that $d = 3$ is the upper critical dimension for the transition. To obtain L_c in this case, one should perform a perturbation expansion in the disorder, as discussed in Ref. [12] in the context of the flux line lattice. One essentially computes the typical displacement u for a system of size $|\mathbf{r}| = L$, which for a LAGB is given by

$$\langle |u(\mathbf{r}) - u(0)|^2 \rangle = \int \frac{d^2 k}{(2\pi)^2} \int \frac{d^2 k'}{(2\pi)^2} (1 - \cos \mathbf{k} \mathbf{r}) G(\mathbf{k}) G(\mathbf{k}') F(\mathbf{k}) F(\mathbf{k}') \quad (31)$$

where $G(\mathbf{k})$ is the Green function associated to the elastic kernel determined in the previous section, and $F(\mathbf{k})$ is the pinning force density. In the spirit of collective pinning theory $\langle F(\mathbf{k})F(\mathbf{k}') \rangle = W\delta^{(2)}(\mathbf{k} + \mathbf{k}')$ with $W = (f_0\sqrt{c_{\text{eff}}\xi_p})^2$. The explicit calculation leads to the characteristic displacement

$$u(L) \simeq f_0\sqrt{c_{\text{eff}}\xi_p} \frac{D^2}{\mu b^2} \ln^{1/2} \frac{L}{D} \quad (32)$$

This expression can then be inverted, imposing $u \sim \xi_p$, to obtain

$$L_c = D \exp \left[\frac{\xi_p}{c_{\text{eff}}} \left(\frac{\mu b^2}{f_0 D^2} \right)^2 \right]. \quad (33)$$

The depinning stress can then be obtained as in $d = 2$ and is given by $\sigma_c b = (\mu b^2 \xi_p) / (DL_c)$. Again these results generalize directly to the pileup case. It is however important to note that they refer to the continuum limit, when one can neglect the discrete nature of the dislocation system. To be consistent with this assumption one should have $L_c \gg D$.

B. Strong pinning: Friedel statistics

Collective pinning is due to a statistical superposition of the forces created by many obstacles. In the limit of strong and/or diluted pinning centers, however, the characteristic bulge of width ξ_p and extension L_c as envisaged in the previous section may not interact with enough pinning centres for this viewpoint to be valid. Simple estimates for the boundaries of the collective pinning regime are given by the inequalities $L_c \xi_p \geq 1/\bar{c}_{\text{eff}}$ and $L_c^2 \xi_p \geq 1/c_{\text{eff}}$ for the $d=2$ and $d=3$ cases discussed above, respectively.

In the regime of strong pinning, dislocations are pinned by individual obstacles. The spacing of obstacles along the dislocation and the depinning stress can be obtained by an argument which was, in the context of single dislocations, developed by Friedel. The basic idea is to consider the behavior of a dislocation segment as it depins from a pair of strong obstacles. The length of the segment is L , and it forms a bulge of width u . If the dislocation segment overcomes one of the pins it will travel by an amount which is, again, of the order of u and, hence, sweep an area of the order of Lu . Now we can estimate the depinning threshold by requiring that during this process the freed dislocation segment encounters, on average, precisely one new obstacle. In other words, precisely at the point of depinning the dislocation starts to move through a sequence of statistically equivalent configurations. For a dislocation this leads to the condition $Lu \simeq 1/(c\xi_p)$. L and u can be related by equating the work done by the external stress σ in bulging out the dislocation to the concomitant elastic energy increase, $\Gamma u^2/L = \sigma buL$, where Γ is a constant line tension. Finally, the depinning force can be

obtained by comparing the external force $b\sigma L$ with the pinning force f_0 . Solving these three equations, one obtains the Friedel length $L_f \simeq (\Gamma/c\xi_p f_0)^{1/2}$ and the depinning stress $\sigma_c b \simeq (c\xi_p f_0^3/\Gamma)^{1/2}$.

This argument can be generalized in a straightforward manner to the case of grain boundaries. Let us first consider the depinning of a two dimensional LAGB as discussed above in the weak pinning limit: In this case, the Friedel condition reads $Lu \simeq 1/\bar{c}_{\text{eff}}$, the elastic energy per unit length of a bulge of width u and extension L is $\mu b^2 u^2/D^2$ which must equal the work per unit length $\sigma bLu/D$, and the force balance (again per unit length) is $\sigma_c bL/D = \bar{f}_0$. Combining these relations we find that the Friedel length and the depinning stress are

$$L_f \simeq \frac{\mu b^2}{D^2 \bar{c}_{\text{eff}} \bar{f}_0} \quad \sigma_c b \simeq \frac{\bar{c}_{\text{eff}} \bar{f}_0^2 D^3}{\mu b^2} \quad (2d). \quad (34)$$

In 3d the Friedel condition is $L^2 u \simeq 1/c_{\text{eff}}$, the energy balance reads $\mu b^2 u^2 L/D^2 = \sigma bL^2 u/D$, and the force balance is $\sigma_c bL^2/D = f_0$. This yields

$$L_f \simeq \frac{\mu b^2}{D^2 c_{\text{eff}} f_0} \quad \sigma_c b \simeq \frac{c_{\text{eff}}^2 f_0^3 D^5}{\mu^2 b^4} \quad (3d). \quad (35)$$

Table 1 presents a compilation of results for the weak and strong pinning cases in two and three dimensions. For comparison we have also included results obtained under the assumption that the elastic behavior of the grain boundary can, in local elasticity approximation, be described by a scale-independent surface energy $\Gamma_0 \sim \mu b^2/D$.

C. Zener pinning in grain growth

From an experimental viewpoint, grain boundary pinning is important since the mobility of grain boundaries may be a limiting factor in grain growth [40, 41]. The dependence of the average grain size R on the impurity concentration c goes under the name of Zener formula and was originally proposed in Ref. [40] and generalized afterwards [41]

$$R \propto c^{-m}, \quad (36)$$

where m is the Zener exponent. Several theoretical and numerical derivations of this formula have been discussed in the literature, often based on the local elasticity approximation [41, 42].

Grain growth is driven by a reduction in energy: For an average grain size R and straight grain boundaries, the characteristic energy stored per unit volume in the form of GB dislocations is of the order of Γ_0/R and, hence, the energy gain achieved by increasing the grain size by dR is $(\Gamma_0/R^2) dR$. Physically, the removal of GB dislocations occurs through the motion of junction points in the GB network. As junction points must drag the connecting GB with them, which may be pinned by disorder, motion

model dimension	type of elasticity	type of pinning	pinning length	critical stress	Zener exponent
2d	local	weak	$L_c = \left(\frac{\Gamma_0^2 \xi_p}{f_0^2 \bar{c}_{\text{eff}}} \right)^{1/3}$	$\sigma_{cb} = \left(\frac{D^3 \bar{f}_0^4 \xi_p \bar{c}_{\text{eff}}^2}{\Gamma_0} \right)^{1/3}$	$m = 2/3$
2d	local	strong	$L_f = \left(\frac{\Gamma_0}{f_0 \bar{c}_{\text{eff}}} \right)^{1/2}$	$\sigma_{cb} = \left(\frac{D^2 \bar{f}_0^3 \bar{c}_{\text{eff}}}{\Gamma_0} \right)^{1/2}$	$m = 1/2$
2d	non-local	weak	$L_c = \frac{\Gamma_0^2 \xi_p}{D^2 \bar{f}_0^2 \bar{c}_{\text{eff}}}$	$\sigma_{cb} = \frac{D^2 \bar{f}_0^2 \bar{c}_{\text{eff}}}{\Gamma_0}$	$m = 1$
2d	non-local	strong	$L_f = \frac{\Gamma_0}{D \bar{f}_0 \bar{c}_{\text{eff}}}$	$\sigma_{cb} = \frac{D^2 \bar{f}_0^2 \bar{c}_{\text{eff}}}{\Gamma_0}$	$m = 1$
3d	local	weak	$L_c = \left(\frac{\Gamma_0^2 \xi_p}{f_0^2 c_{\text{eff}}} \right)^{1/2}$	$\sigma_{cb} = \frac{D f_0^2 c_{\text{eff}}}{\Gamma_0}$	$m = 1$
3d	local	strong	$L_f = \left(\frac{\Gamma_0}{f_0 c_{\text{eff}}} \right)^{1/2}$	$\sigma_{cb} = \frac{D f_0^2 c_{\text{eff}}}{\Gamma_0}$	$m = 1$
3d	non-local	weak	$L_c = D \exp \left[\frac{\Gamma_0^2 \xi_p}{D^2 f_0^2 c_{\text{eff}}} \right]$	$\sigma_{cb} = \frac{\Gamma_0 \xi_p}{D} \exp \left[-\frac{\Gamma_0^2 \xi_p}{D^2 f_0^2 c_{\text{eff}}} \right]$	exponential
3d	non-local	strong	$L_f = \frac{\Gamma_0}{D f_0 c_{\text{eff}}}$	$\sigma_{cb} = \frac{D^3 f_0^3 c_{\text{eff}}^2}{\Gamma_0^2}$	$m = 2$

TABLE I: Overview of pinning stresses and pinning lengths obtained from different models

can only occur if the energy gain at least matches the dissipative work which has to be done against the pinning forces. The dissipative work per unit volume expended in moving all GB by dR is $\sigma_{cb}/(DR)dR$, and balancing against the energy gain yields the limit grain size

$$R_l \approx \frac{\Gamma_0 D}{\sigma_{cb}} \approx \frac{\mu b}{\sigma_c}. \quad (37)$$

According to this relation, the grain size is inversely proportional to the pinning stress. This gives a possibility to experimentally assess the nature of the pinning by ‘tuning’ the pinning stress and measuring the grain size as a function of the tuning parameters.

An obvious method to tune the pinning stress is to modify the concentration of the pinning centers and to measure the impact this has on grain size [40]. However, this requires the comparison of results from different samples and experimental results reported in the literature are inconclusive [41, 49, 50]. We therefore refer to a quite different and unusual type of grain growth experiment where the configuration of the pinning obstacles is kept constant but the properties of the lattice are changed.

This type of grain growth experiment may be carried out on vortex lattices of type-II superconductors in which quasi two-dimensional grain structures are observed in (vortex polycrystals). In such a system an external magnetic field penetrating the sample forms flux lines that are disposed in a triangular lattice, whose elastic properties (namely the lattice spacing and the elastic moduli) depend on the magnetic field itself. A detailed theory of grain growth in vortex polycrystals [53] can be developed along the same lines followed here. In this case, it is worth pointing out that the agreement of the theory with magnetic decoration data for the average grain size is quite satisfactory, especially if compared to the estimate based on local elasticity assumptions.

IV. DYNAMICS: CRITICAL SCALING NEAR THE DEPINNING THRESHOLD

Second-order phase transitions can be described by scaling laws and critical exponents and the depinning transition is no exception. In the system discussed here, the control parameter is the applied stress, so that scaling laws depend on the distance from the critical point $\sigma - \sigma_c$. In particular, as the system approaches the transition the correlation length diverges as $\xi \sim (\sigma - \sigma_c)^{-\nu}$. Similarly, one can define a characteristic correlation time t^* , related to the correlation length as $t^* \sim \xi^z$. The average dislocation velocity reaches a steady value, scaling as $v \sim (\sigma - \sigma_c)^\beta$, above the transition, and vanishes below. Before the steady-state the average velocity decays as a power law $t^{-\theta}$, for times $t < t^*$. Furthermore, the Orowan relation, a phenomenological law which relates the rate of plastic deformation $\dot{\gamma}$ to average values of moving dislocations density and velocity in a given crystal, implies that similar scaling laws should hold for the strain rate $\dot{\gamma} \equiv b \rho v$, where ρ is the density of moving dislocations, and v their average velocity. In this respect, it is thus tempting to establish a relationship between dynamical behavior and the creep laws observed in plastically deforming crystals, i.e. the crossover between primary (power law) to secondary (linear) creep, due to their resemblance.

Scaling exponents also characterize the morphology of the dislocation arrangement, which exhibits roughening close to the depinning transition. The roughness can be quantified measuring the average displacement correlations $C(x - x') = \langle (u(x) - u(x'))^2 \rangle$. At the transition in the steady-state, we expect a self-affine scaling $C(x) \sim x^{2\zeta}$, where ζ is the roughness exponent while the transient behavior is described by a scaling form of the type $C(x, t) = t^{\beta_t} f(x/t^{1/z})$. As in ordinary critical phenomena, only a fraction of the scaling exponents are independent. For instance, one can easily derive the relations $\beta_t = z/\zeta$ and $\theta = \beta/(vz)$.

In general, it has been shown that in the depinning

problem there are only two independent exponents that have been computed using the renormalization group. To connect our problem to previously obtained results, we notice that the effective elastic energy of the pileup and LAGB scales as $|q|$ in Fourier space, as in the problems of contact line [51] and planar crack depinning [52]. We can thus directly apply to our case the results obtained for a manifold with long-range elastic energy [14, 26]. The renormalization group analysis predicts that $d_c = 3$ is the upper critical dimension, above which fluctuations are suppressed. Thus for $d > d_c$ there is no roughening (i.e. $\zeta = 0$) and the other exponents can be computed in the mean-field approximation, yielding $\beta = z = \nu = 1$. These results are valid in the physically interesting dimension $d = 3$ apart from additional logarithmic corrections. For $d < 3$, a renormalization group expansion in $\epsilon = 3 - d$ has been performed to compute the exponents which at first order in ϵ are given by $\beta = 7/9$, $\nu = 3/2$, $\zeta = 1/3$ and $z = 7/9$ [26]. Using the scaling relation $\theta = \beta/(\nu z)$ one obtains $\theta = 2/3$, which coincides with the exponent of the so-called Andrade creep law, observed in the creep deformation of several materials [13, 43].

A. Two-dimensional pileup: Numerical simulations

In order to test the validity of the theoretical results, we have performed a series of numerical simulations for the dynamics of a two-dimensional pileup. This corresponds to an effective one dimensional model in which N interacting point dislocations move along a line in presence of quenched disorder. For simplicity we consider periodic boundary conditions, so that in absence of disorder the equilibrium configuration is an equally spaced pileup. To test the dependence on the system size, we change the dislocation number N and the system size L keeping the dislocation spacing $D = L/N$ constant.

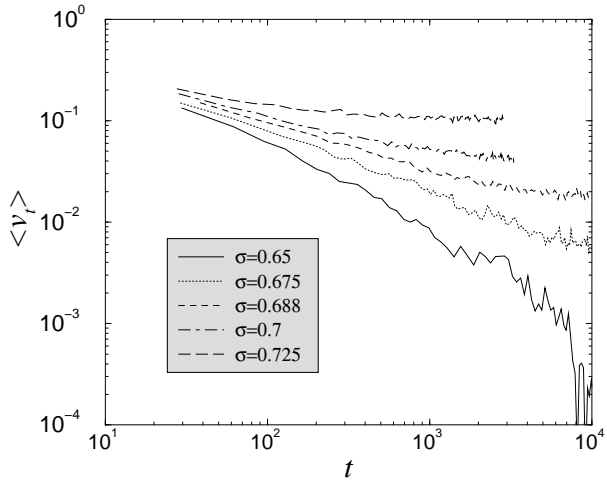


FIG. 4: The decay of the average pileup velocities as a function of the applied stress σ . For $\sigma > \sigma_c \simeq 0.675$ the velocity reaches a steady value and decays to zero otherwise.

The equation of motion for the dislocation i in the pileup is given by

$$\chi \frac{dx_i}{dt} = \mu b^2 \sum_{j \neq i} \frac{1}{|x_i - x_j|} + b\sigma + \sum_P f_p(x_i - X_P), \quad (38)$$

where χ is an effective viscosity and σ is the applied stress. The pinning centers are placed at randomly chosen positions X_P (with $P = 1, \dots, N_P$) and exert an attractive force on the dislocations

$$f_p(x) = -f_0 \frac{x}{\xi_p} e^{-(x/\xi_p)^2}. \quad (39)$$

In order to correctly take into account the effect of periodic boundary conditions the interactions between dislocations are summed over the images. In one dimension the sum can be performed exactly and $1/|x|$ in Eq. 38 is replaced by

$$\sum_{k=-\infty}^{\infty} \frac{1}{x + kL} = \frac{\pi}{L \tan(\pi x/L)}. \quad (40)$$

The equation of motion (Eq. 38) is integrated numerically using a Runge-Kutta algorithm for different values of the applied stress. We take as initial condition a perfectly ordered pileup, with equally spaced dislocations. For the simulations reported here, we first considered $N = 64, 128, 256, 512$ dislocations with a spacing $D = 16$ and average pinning center spacing $d_p \equiv L/N_p = 2$. The units of time, space, and forces are chosen so that $\mu b^2 = 1$, $\chi = 1$, and $b = 1$, and we set $f_0 = 1$ and $\xi_p = 1$.

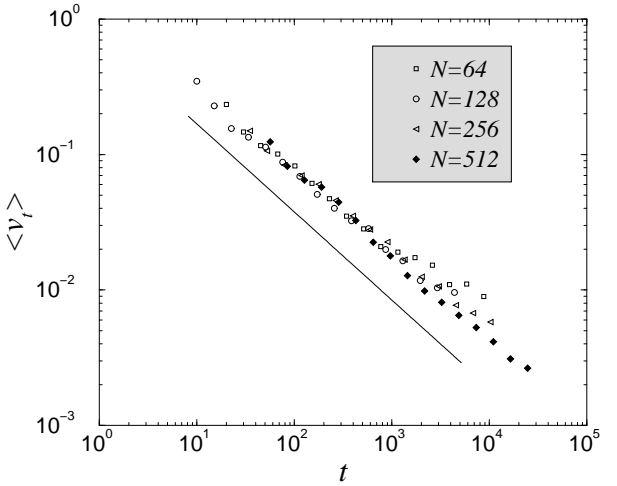


FIG. 5: The decay of the velocity at $\sigma > \sigma_c \simeq 0.675$ for different values of N . As N increases the power law scaling region extends. The line has a slope of $\theta = 0.65$.

In Fig. 4 we report the time decay of the average pileup velocity for different values of the applied stress. For large stress values, $\sigma > \sigma_c \simeq 0.675$, the initial power law decay is followed by a plateau, while the velocity decays to zero otherwise. This allows to identify the depinning

point as $\sigma_c \simeq 0.675$. This is confirmed by the finite size analysis shown in Fig. 5, indicating that for $\sigma_c = 0.675$ the power law extends further as the system size is increased. The exponent of the power law scaling $\theta \simeq 0.65$ is in good agreement with the theoretical expectations.

Moreover, in order to characterize the growth of correlations at the critical point, we compute the displacement correlation function $C(i-j, t) = \langle (u_i(t) - u_j(t))^2 \rangle^{1/2}$ at different times t for $\sigma = \sigma_c$ (see Fig. 6). The curves can be collapsed using the scaling form $C(x, t) = t^{\zeta/z} f(x/t^{1/z})$ with $\zeta = 0.35$ and $z = 0.9$ (see the inset of Fig. 6). To confirm this result we have also computed the evolution of the power spectrum $P(k, t) = \int dx C(x) \exp(ikx)$. These curves can also be collapsed as $P(k, t) = t^{(2\zeta+1)/z} g(kt^{1/z})$ with the same exponent values as the correlation function.

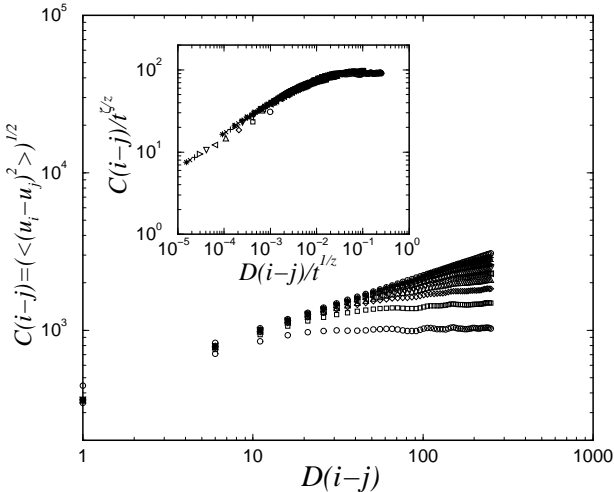


FIG. 6: The growth of the correlation function at the depinning transition at different times. The data collapse in the inset allows to estimate the roughness exponent $\zeta = 0.35$ and the dynamic exponent $z = 0.9$.

In summary, all the exponents determined from the simulations are in good agreement with the renormalization group predictions and with previous simulations based directly on the elastic approximation, confirming the validity of the elastic theory for the pileup.

B. Three-dimensional pileup: relaxation of slip-band growth rates

Direct experimental observation of the velocity relaxation behavior of planar dislocation arrangements is possible in certain alloys exhibiting so-called planar slip where dislocations may form huge pile-ups (see Figure 1). The motion of these planar dislocation groups goes along with the formation of large slip steps along the traces where the slip plane of the pileup intersects the surface of the metal specimen. For a moving pile-up consisting of roughly equally spaced dislocations, the slip step growth

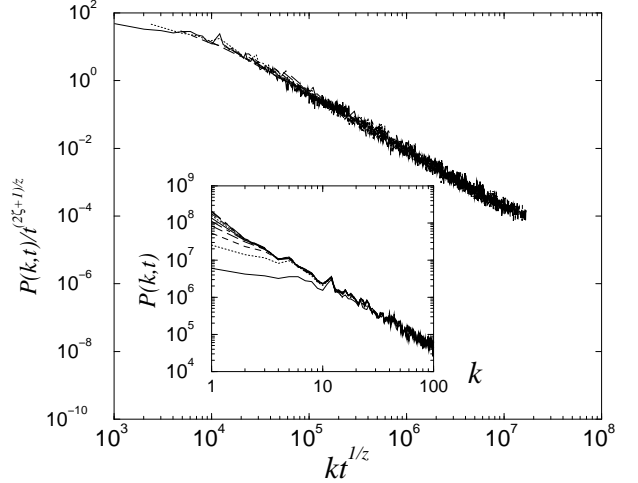


FIG. 7: The power spectrum of the pileup at the depinning transition. The data collapse is consistent with the scaling of the correlation function.

rate is proportional to the dislocation velocity. Since the slip step growth rate can be directly observed, this gives a possibility for a direct experimental check of theoretical predictions.

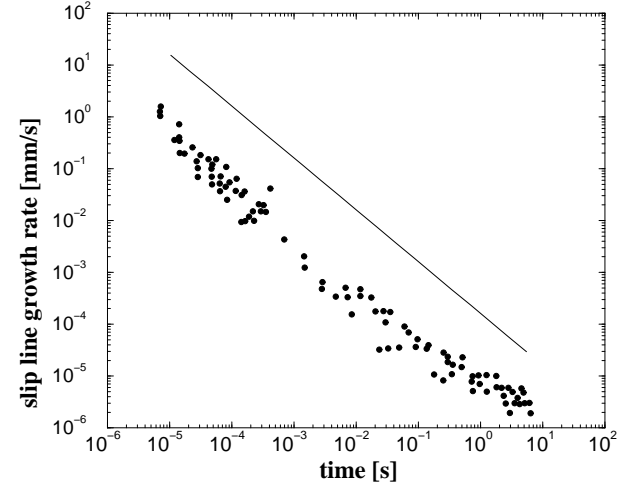


FIG. 8: Growth rate of slip steps on the surface of Cu-30at% Zn deformed at room temperature as a function of the time passed after growth has started; after Ref. [9]. The line is a power law with exponent $\theta = 1$.

Figure 8 shows observed rates of slip step growth as a function of the time after growth has started. The double-logarithmic plot indicates relaxation of the growth rate (the dislocation velocity) according to $v \propto t^{-\theta}$ with a characteristic exponent $\theta = 1 \pm 0.1$ over six decades. This indicates that the power-law is related to a depinning transition of planar dislocation arrays in 3D for which we expect mean-field exponents (see above) and according to the scaling relation $\theta = \beta/(\nu z)$ a value

$\theta = 1$. The apparent length of the scaling regime indicates that driving of the dislocation arrays occurs at stresses very close to the critical one. This is in line with the general observation that dislocation arrangements in slowly deforming crystals (where 'slow' covers the entire range of strain rates used in typical experiments, [54]) are in a close-to-critical state [54, 55].

V. CONCLUSIONS

We have investigated the depinning transition of planar dislocation arrays such as small-angle grain boundaries or dislocation pile-ups. Contrary to the case of isolated dislocations, the elastic interactions between dislocation line segments in such arrays are of long-range nature and, hence, cannot be described within a line- or surface-tension approximation. The pinning of planar dislocation arrays has been investigated both in the weak and strong pinning limits using collective pinning theory and Friedel statistics, respectively. The results have been applied to the problem of grain growth limited by grain boundary pinning referred to as Zener pinning.

Long-range elastic interactions also govern the dynamics of planar dislocation arrays at the depinning threshold. In two dimensions, computer simulations and theoretical arguments suggest that the dynamics falls into the same class as contact-line depinning, while in three dimensions the dynamical behavior can be described by mean-field exponents. In particular, we have demon-

strated that the mean-field prediction for the velocity relaxation of a planar dislocation array (pile-up) is consistent with experimental observations of the time-dependent growth of slip bands in alloys exhibiting planar slip.

The dislocation arrangements discussed in the present study have a simple, quasi-planar geometry in which only dislocations of one sign are present and only small perturbations of the planar arrangement of the dislocations are permitted. Because of this particular geometry, the dislocation assemblies behave like two or three-dimensional long-range elastic manifolds. The situation is much more complicated when dislocations of different types and directions of motion have to be considered. In such situations, there is still a transition between a stationary and a moving state of the dislocation assembly ('yielding transition'). However, in general dislocation assemblies the existence of metastable stationary states does not depend on the presence of quenched disorder as in the present study. Rather, the interactions between dislocation lines of different type together with the dynamics constraints which tie the motion of the dislocation lines to their respective slip planes lead to the possibility of forming metastable jammed configurations even in the absence of any disorder. While the general scenario of dynamic non-equilibrium phase transitions applies to such systems, no ready-made theoretical framework is available and, hence, a theory of the yielding and dynamic behavior of general dislocation systems remains a formidable task for future investigations.

[1] F. R. N. Nabarro, Proc. R. Soc. Lond. A **381**, 285 (1982).
 [2] E. H. Brandt, Phys. Rev. Lett. **56**, 1381 (1986).
 [3] L. B. Ioffe and V. M. Vinokur, J. Phys. C **20**, 6149 (1987).
 [4] J. G. Sevillano, E. Bouchaud and L. P. Kubin, Scr. Metall. Mater. **25**, 355 (1991).
 [5] G. D'Anna, W. Benoit and V. M. Vinokur, J. Appl. Phys. **82**, 5983 (1997).
 [6] S. Zapperi and M. Zaiser, Mat. Sci. and Eng. A **309-310**, 348 (2001).
 [7] F. R. N. Nabarro (ed.), *Dislocations in Solids*, Vol. 4, (North-Holland, Amsterdam, 1979).
 [8] M. Z. Butt and P. Feltham, J. Mat. Sci. **28**, 2557 (1993).
 [9] H. Neuhauser, Phys. Scr. **T49** 412 (1993).
 [10] R. Labusch, Phys. Status Solidi **41**, 659 (1970); Acta Metall. **20**, 917 (1972).
 [11] R. Labusch, Cryst. Lattice Defects **1**, 1 (1969).
 [12] A. I. Lar'kin and Yu. N. Ovchinnikov, J. Low Temp. Phys. **34**, 409 (1979).
 [13] J. Friedel, *Dislocations* (Pergamon Press, Oxford, 1967).
 [14] M. Kardar, Phys. Rep. **301** 85 (1998).
 [15] S. Lemerle, J. Ferré, C. Chappert, V. Mathet, T. Gihamachi, and P. Le Doussal Phys. Rev. Lett. **80**, 849 (1998).
 [16] S. Zapperi, P. Cizeau, G. Durin and H. E. Stanley, Phys. Rev. B **58**, 6353 (1998).
 [17] S. Bhattacharya and M. J. Higgins, Phys. Rev. Lett. **70**, 2617 (1993).
 [18] R. Surdeanu, R. J. Wijngaarden, E. Visser, J. M. Huijbregtse, J. H. Rector, B. Dam, and R. Griessen Phys. Rev. Lett. **83**, 2054 (1999).
 [19] E. Schäffer and P.-z. Wong Phys. Rev. E **61**, 5257 (2000).
 [20] E. Rolley, C. Guthmann, R. Gombrowicz, and V. Repain Phys. Rev. Lett. **80**, 2865 (1998).
 [21] E. Bouchaud, J Phys. C **9**, 4319 (1997).
 [22] J. Schmittbuhl and K. Måløy, Phys. Rev. Lett. **78**, 3888 (1997).
 [23] T. Nattermann, S. Stepanow, L. H. Tang, and H. Leschhorn J. Phys. II (France) **2**, 1483 (1992).
 [24] H. Leschhorn, T. Nattermann, S. Stepanow, and L. H. Tang, Ann. Physik **6**, 1 (1997).
 [25] O. Narayan and D. S. Fisher, Phys. Rev. B **48**, 7030 (1993).
 [26] D. Ertas and M. Kardar, Phys. Rev. E **49**, R2532 (1994).
 [27] P. Chauve, T. Gihamachi, and P. Le Doussal Phys. Rev. B **62**, 6241 (2000).
 [28] P. Le Doussal, K. J. Wiese, and P. Chauve Phys. Rev. B **66**, 174201 (2002).
 [29] D. Cule and T. Hwa, Phys. Rev. Lett. **77**, 278 (1996); Phys. Rev. B **57** 8235 (1998).
 [30] F. Lacombe, S. Zapperi and H. J. Herrmann, Phys. Rev. B **63**, 104104 (2001).
 [31] A. Rosso, A. K. Hartmann, and W. Krauth Phys. Rev. E **67**, 021602 (2003).
 [32] J. Schmittbuhl, S. Roux, J.P. Villotte, and K. J. Maloy,

Phys. Rev. Lett. **74**, 1787 (1995).

[33] S. Ramanathan and D. Fisher, Phys. Rev. Lett. **79**, 877 (1997); Phys. Rev. B **58**, 6026 (1998).

[34] A. Tanguy, M. Gounelle and S. Roux, Phys. Rev. E **58**, 1577 (1998).

[35] A. Rosso and W. Krauth Phys. Rev. E **65**, 025101 (2002).

[36] A. J. E. Foreman, Phil. Mag. **15**, 1011 (1967).

[37] G. De Wit and J. S. Koehler, Phys. Rev. **116**, 1113 (1959).

[38] G. Blatter *et al.*, Rev. Mod. Phys. **66**, 1125 (1994).

[39] M.C. Miguel and M. Kardar, Phys. Rev. B **56**, 11903 (1997).

[40] C. S. Smith, Trans. AIME **175**, 15 (1948).

[41] P. A. Manohar, M. Ferry and T. Chandra, ISIJ Intern. **38**, 913 (1998)

[42] P. M. Hazzledine and R. D. J. Oldershaw, Phil. Mag. A **61**, 579 (1990).

[43] M.C. Miguel, A. Vespignani, M. Zaiser and S. Zapperi, Phys. Rev. Lett. **89**, 165501 (2002).

[44] J. Plessing, PhD thesis, University of Braunschweig 1995.

[45] S. I. Zaitsev and E. M. Nadgorny, Sov. Phys. Solid State **21**, 804; *ibid* 1934 (1979).

[46] J.P. Hirth and J. Lothe, Theory of Dislocations (McGraw Hill, New York, 1968).

[47] An analogous expression was derived in S. T. Chui, Phys. Rev. B **28**, 178 (1983).

[48] Because of the emergence of ‘corners’ in the dislocation lines, this yields a rather poor description of the interaction between adjacent line segments. However, in the following we are mainly interested in the long-wavelength elasticity of the dislocation lines, which in this staircase approximation is captured exactly in the limit of infinitesimally small segment lengths.

[49] D.L.Olgaard and B. Evans, J. Am. Ceram. Soc. **69**, C-272 (1986).

[50] M. Miodownik M, E.A. Holm and G.M. Hassold, Scripta Mater. **42**, 1173 (2000).

[51] J.F. Joanny and P.G. de Gennes, J. Chem. Phys. **81**, 552 (1984).

[52] H. Gao and J. R. Rice, ASME J. Appl. Mech. **56**, 828 (1989).

[53] P. Moretti, M.-C. Miguel, M. Zaiser and S. Zapperi, (submitted).

[54] M.Zaiser, Mater. Sci. Engng. A **309/310**, 304 (2001).

[55] M.-C. Miguel, A. Vespignani, S. Zapperi, J. Weiss and J. R. Grasso, Nature **410**, 667 (2001).